The X-Ray Crystallographic Structure of the Human Neonatal Fc Receptor at Acidic pH Gives Insights into pH-Dependent Conformational Changes

Mohammed Taha[a], E. Sally Ward[b] and Hyun-Joo Nam*[a]

[a]Department of Bioengineering, The University of Texas at Dallas, Richardson, TX 75080, USA; [b]Department of Molecular and Cellular Medicine and Department of Microbial Pathogenesis and Immunology, Texas A&M Health Science Center, College Station, TX 77840, USA

*Corresponding author:
Hyun-Joo Nam
University of Texas at Dallas, 800 W. Campbell Road RL10, Richardson, TX, 75080, United States
Tel: 1-972-883-5786
Fax: 1-972-883-4653
email: hnam@utdallas.edu

Running Title: hFcRn, low pH apo structure

Abstract:

High levels of circulating immunoglobulin G (IgG) and serum albumin (SA) are maintained through recycling by the neonatal Fc receptor (FcRn). FcRn interacts with IgG and SA in a pH-dependent manner and rescues them from lysosomal degradation. We have determined the crystal structure of extracellular domain of human FcRn, a heterodimeric complex of α-chain and β2¬microglobulin, at pH 4.5. The structure was compared with the previously reported unliganded human FcRn structure at pH 8.5 and complex structures of FcRn bound to SA and/or Fc determined at acidic pHs. Structural differences are more pronounced between the two unliganded FcRn structures at pH 4.5 and pH 8.5 than between unliganded FcRn and the complex structures at acidic pHs. At acidic pH, protonation of H166 induces interactions with E54 and Y60 stabilizing the "WW loop" important for SA binding, and H161 interacts with E165 causing con-formational changes of helix 3. These structural changes make the FcRn amenable for binding with SA at acidic pH. The Fc binding surface does not show any major main chain differences between the unliganded structures at pH 8.5 and pH 4.5. Side chain changes upon Fc binding were observed when compared with the complex structures. This suggests that major structural differences observed between the unliganded and ligand bound structures are primarily due to pH changes rather than ligand binding.

Keywords: Human neonatal Fc receptor, β2-microglobulin, Human Serum Albumin, FcRn, Antibody Recycling, pH dependent binding.

INTRODUCTION

The neonatal Fc receptor (FcRn) plays key roles in pro-viding passive immunity transferred from mother to the off-spring and maintaining immunoglobulin G (IgG) and albu-min concentrations in the body [1-3]. FcRn is a heterodimer composed of a heavy chain (α-chain) and β2-microglobulin (β2m) [4]. The N-terminal segment of the α-chain and the non-covalently associated β2m comprise the extracellular portion, and the C-terminal segment of the heavy chain constitutes the transmembrane region and a relatively short cytoplasmic domain [5, 6].

FcRn interacts with serum albumin (SA) and the Fc seg-ment of IgG through separate interacting surfaces in a pH dependent manner [7-9]. SA and IgG bind to FcRn at acidic pH (< 6.5) in endosomal compartments, and then are sorted back to the cell surface and released at higher, physiological pH [10]. Since FcRn rescues its ligands from lysosomal de-radation and increases their in vivo half-lives, the pH-dependent interaction with FcRn forms an engineering focus for Fc- and albumin-based therapeutics.

Several structural studies of FcRn were previously reported and led to a molecular understanding of the pH-dependent interactions with SA and Fc. Among them, the human FcRn (hFcRn) structure in the unliganded form was determined at pH 8.5, and the structures of complexes of hFcRn with human SA (hSA) or an immunoglobulin Fc fragment were all determined at pH 4.0~5.2 [4, 8, 11-13]. In addition, the structure of hFcRn bound to a peptide inhibitor was determined at pH 4.2 [14]. Currently, the structure of unliganded hFcRn at the low pH range is unavailable for comparison with the complex structures.

In the current study we have determined the crystal structure of unliganded hFcRn at pH 4.5. The atomic coordinates and the structural factors are deposited in the Protein Data Bank as entries 5BXF. This structure has been compared with the structures of unliganded hFcRn at pH 8.5 and complexes of hFcRn bound to hSA or Fc.

MATERIALS AND METHOD

Production of Human FcRn

The baculovirus expression construct for the extracellular domain of hFcRn has been previously reported [15]. Minor modifications were made to the purification protocol to improve the yield

and purity of the protein. The expressed α-chain containing the extracellular portion of α-chain (residues 24-290) and a C-terminal 6-histidine tag was coexpressed with β2-microglobulin in High Five™ cells (Life Technologies) at 28°C. The protein was secreted into the media and was harvested at 3.5 days after the baculovirus infection.

The cell debris was pelleted by centrifugation at 8200 g for 30 minutes and discarded. The supernatant containing secreted protein was filtered using a 0.8 μm membrane filter (Whatman), and dialyzed for two days in phosphate buffered saline (PBS), pH 7.2 at 4 °C using the dialysis membrane with the molecular weight cut off (MWCO) limit of 3.5 kDa (Fisherbrand). Human FcRn protein was first purified by standard affinity chromatography using Ni-NTA agarose. The dialyzed sample was loaded onto the column, and the column was washed with buffers A, B and C. Buffer A consisted of 20 mM Tris pH 7.2, 150 mM NaCl; Buffer B, 20 mM Tris pH 7.2, 150 mM NaCl, 20 mM Imidazole; and Buffer C, 20 mM Tris pH 7.2, 150 mM NaCl, 40 mM Imidazole. The protein was eluted using the elution buffer containing 20 mM Tris pH 7.2, 150 mM NaCl, and 250 mM Imidazole. Fractions containing hFcRn were combined and concentrated using Amicon Ultra-15 (Millipore) with 10 kDa MWCO. The protein was further purified by size-exclusion chromatography using a Superdex 75 column (GE Healthcare) equilibrated in 20 mM Tris pH 7.2, 150 mM NaCl. Throughout the purification steps, eluted fractions were analyzed using SDS-PAGE. The protein peak fractions were combined, concentrated using Amicon Ultra -15 (10 kDa) to the final concentration of 25 mg/ml and stored at ¬80°C.

Crystallization, Data Collection and Processing

The sparse-matrix method was used to screen the crystallization conditions. The crystals were obtained from hanging drops consisted of 1μl protein solution mixed with 1μl reservoir solution containing 0.1M Sodium Citrate pH 4.5, 20% (w/v) PEG 4000. Crystals were harvested and soaked in the cryoprotectant solution composed of 0.1 M Sodium Citrate pH 4.5, 20% PEG 4000, and 25% Glycerol, and flash-cooled in liquid nitrogen. X-ray diffraction data were collected at the A1 beamline of the Cornell High Energy Synchroton Source (CHESS) using an ADSC Quantum 210 CCD detector. Crystal-to-detector distance was set at 225 mm, and an oscillation angle of 1° and a 15 second exposure time per image were used. HKL-2000 suite was used to index and process the data [16]. For additional analyses, programs from Phenix suite were used [17].

Structure Solution, Refinement and Analyses

The structure was determined using molecular-replacement and unliganded hFcRn at pH 8.5 (PDB ID: 1EXU) [12] as the model and the program Phaser [18]. Structure refinement and analyses were performed using the programs from Phenix suite [17] and COOT [19]. Geometric calculations and figures were made using Procrustes Structural Matching Alignment and Restraint Tool (ProSMART) in CCP4mg [20] and PyMOL [21].

RESULTS AND DISCUSSIONS

Overall Structure of Human FcRn at pH 4.5

The extracellular portion of the hFcRn, composed of the α-chain and β2m, was crystallized with 2 heterodimeric complexes in an asymmetric unit. The crystal diffracted to 2.85 Å and all of the β2m and all of the α-chain residues were assigned to well-defined densities with the exception of the three N-terminal residues (Table 1). No ordered sugar moiety was observed in the structure. The two αβ2m complexes are related by 180° rotation and show identical conformations with the C_α rmsd of 0.64 Å (Figure 1). As noted previously, FcRn is structurally similar to class I major histocompatibility complex (MHC-I) molecules and includes a non-functional peptide binding groove with narrow helical walls (Figure 1) [4, 14].

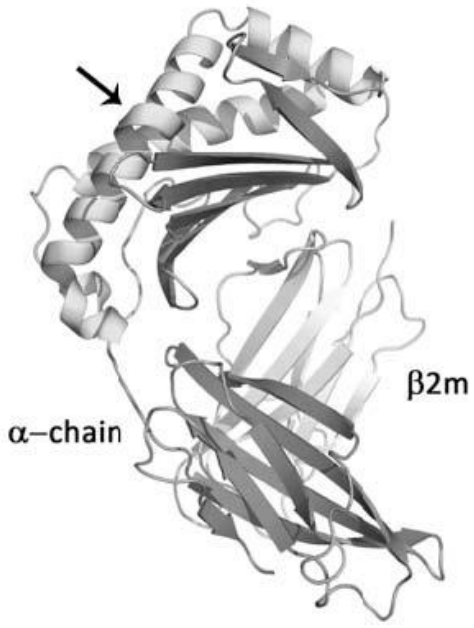

Figure 1. Schematic representation of the structure of hFcRn determined at pH 4.5. The heterodimeric complex composed of the α¬chain and β2m is shown with the non-functional peptide binding groove (arrow).

Table 1. Data collection and refinement statistics.

Data Collection	
Space group	$P2_1$
Unit cell	a=42.18 Å, b=77.58 Å, c=140.55Å, β=93.60°
Resolution range (Å)	46.76–2.85 (2.95-2.85)
No. of unique reflections	21220 (2037)
Multiplicity	4.1 (4.2)
Completeness (%)	99.6 (100)
Average I/σ	12.0 (3.0)
$R_{meas.}$ (%)	0.155 (0.634)
Refinement	
R_{cryst} / R_{free}	0.24/0.31
No. of non-H atoms	
Protein	5797
Water	1
Total	5798
R.m.s. deviations	
Bonds (Å)	0.010
Angles (°)	1.554
Average *B* factors (Å^2)	
Protein	45.9
Ramachandran plot	
Most favoured (%)	89.11
Allowed (%)	8.24

$R_{meas,}$ the multiplicity-weighted R_{merge} [22]

Comparisons of human FcRn structures

The current structure of hFcRn at pH 4.5 (a-hFcRn: acidic hFcRn) was compared with that for hFcRn at pH 8.5 (b-hFcRn: basic hFcRn) (PDB ID: 1EXU), the hFcRn-hSA, hFcRn-hSA-Fc, and hFcRn-peptide inhibitor complex structures (PDB ID: 4K7I, 4N0U and 3M1B, respectively). The complex structures were all determined at acidic pHs. Structural comparisons show very close conformations among them with C_α rmsd of 0.95 Å between the a-hFcRn and b-hFcRn, and 0.63~0.79 Å between the a-hFcRn and the com-plex structures. Greater conformational differences were observed between the a-hFcRn and b-hFcRn than between the a-hFcRn and the complexes. This indicates that the con-formational differences observed between the b-hFcRn and the complex structures are mainly attributed to pH-dependent changes rather than induced by ligand binding.

The main chain differences among the acidic pH structures, a-hFcRn and the complexes, are limited only to loop regions (Figure 2A). Most of the loop regions are involved in

crystallographic and non-crystallographic contacts, and functional implications of the variable conformations are not clear. When a-hFcRn and b-hFcRn are compared, main chain differences were observed at the third helix (Helix 3) and the "WW loop" involve in interactions with hSA (Figure 2B) (17; 13). The low pH-induced ordering of "WW loop" (residues 52-60) is mediated by H166 as previously described (17). The ordered "WW loop" creates a hydrophobic interface comprising the major hSA interaction motif. Protonation of H166 and additionally H161 at acidic pH also induces structural changes in the third helix. At pH 4.5, the N_ atom of H166 interacts with the terminal carboxyl group of E54, and the H161 N_ atom with E165 (Figure 2B). These interactions cause greater than 1 Å of displacement of Helix 3 toward the C-terminal direction of the helix compared with the pH 8.5 structure.

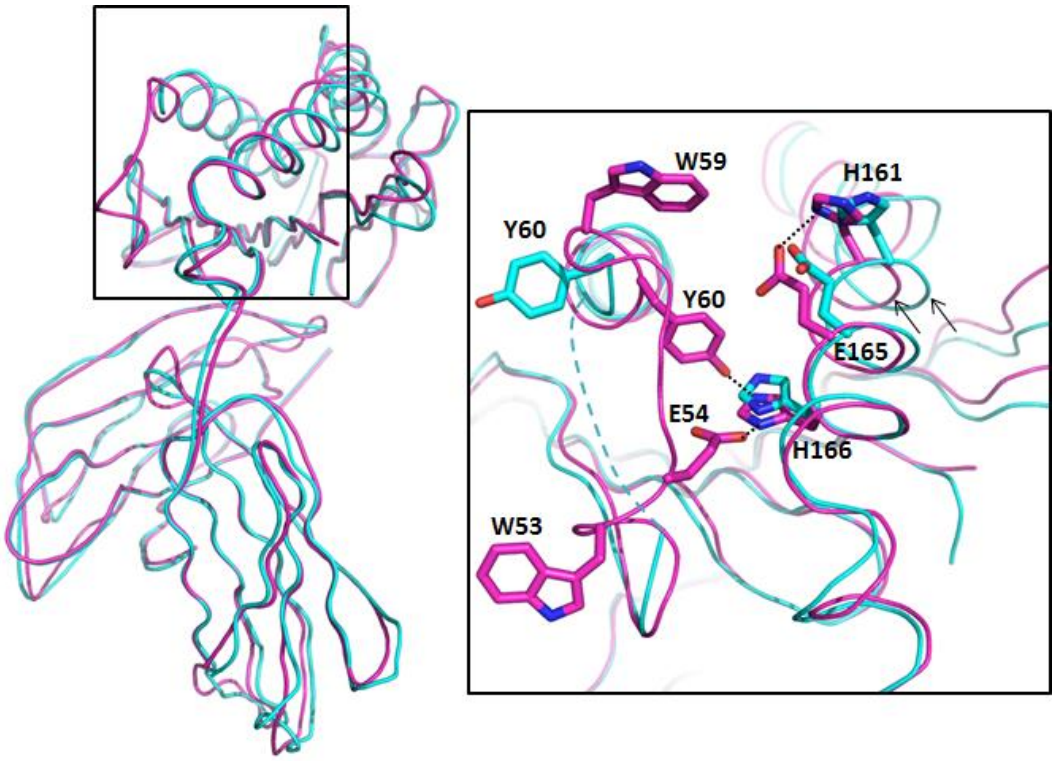

Figure 2. Structural comparisons of a-hFcRn and b-hFcRn. A. Superimposition of the structures of unliganded FcRn at pH 4.5 (magenta) and pH 8.5 (cyan). The boxed regions indicate the main chain variations observed at helix 3 and the "WW loop". B. Zoomed-in view of the boxed area shown in panel A. Side chains involved in hydrogen bonds at pH 4.5 are shown. The disordered "WW loop" at pH 8.5 is illustrated as a dotted line in cyan. Hydrogen bonds are shown with black dotted lines. The pronounced differences in helix 3 between the structures at basic and acidic pH is indicated by arrows.

Helix 3 is involved in intermolecular contacts with hSA and the change at low pH is optimal for the interactions. When superimposed with the FcRn-hSA complex structures, the low pH structure is maintained in all of the complex structures. To understand the pH-dependent dissociation at high pH, a composite model of b-hFcRn (PDB ID: 1EXU) was superimposed onto FcRn in the complex structure (PDB ID: 4N0U) (Figure 3). With b-hFcRn, steric hindrance was observed between hFcRn F157 and hSA residues 81-84 (Figure 3B). Additionally, the interactions between O_ of T153 of hFcRn and E86 of hSA were disrupted in the high pH complex model. Although helix 3 comprises only a mi¬nor interaction surface between hFcRn and hSA, the structural analysis presented here postulates a contribution by the helix for the pH-dependent transition. The high pH hFcRn conformation produces steric clash with hSA and may trigger dissociation at physiological pH.

Interactions between FcRn and Fc are mediated through residues E115/E116/ E133 of the hFcRn αchain and residues located at the CH2-CH3 domain interface of Fc (13). When the high and low pH unliganded structures and the complex structures were compared, FcRn models primarily show conformational changes in side chains. These differences were more pronounced between the unliganded and complex structures at low pH values rather than between unliganded structures of different pHs (Figure 3C). This implies that ligand binding induces the side chain changes at the Fc-FcRn interaction interface, rather than the pH transition.

CONCLUSION

The structure of unliganded FcRn at pH 4.5 presented here confirms that the main chain structural differences observed between the high pH structure and the complex structure determined at acidic pH are attributed to pH changes rather than induced by binding. Our analysis shows that the pH-dependent hFcRn-hSA interaction is affected by the structural changes which may explain the pH-dependence of has binding. The structure of FcRn at pH 4.5 reported here will help to provide basis for albumin and Fc based therapeutics, the intensely pursued research areas.

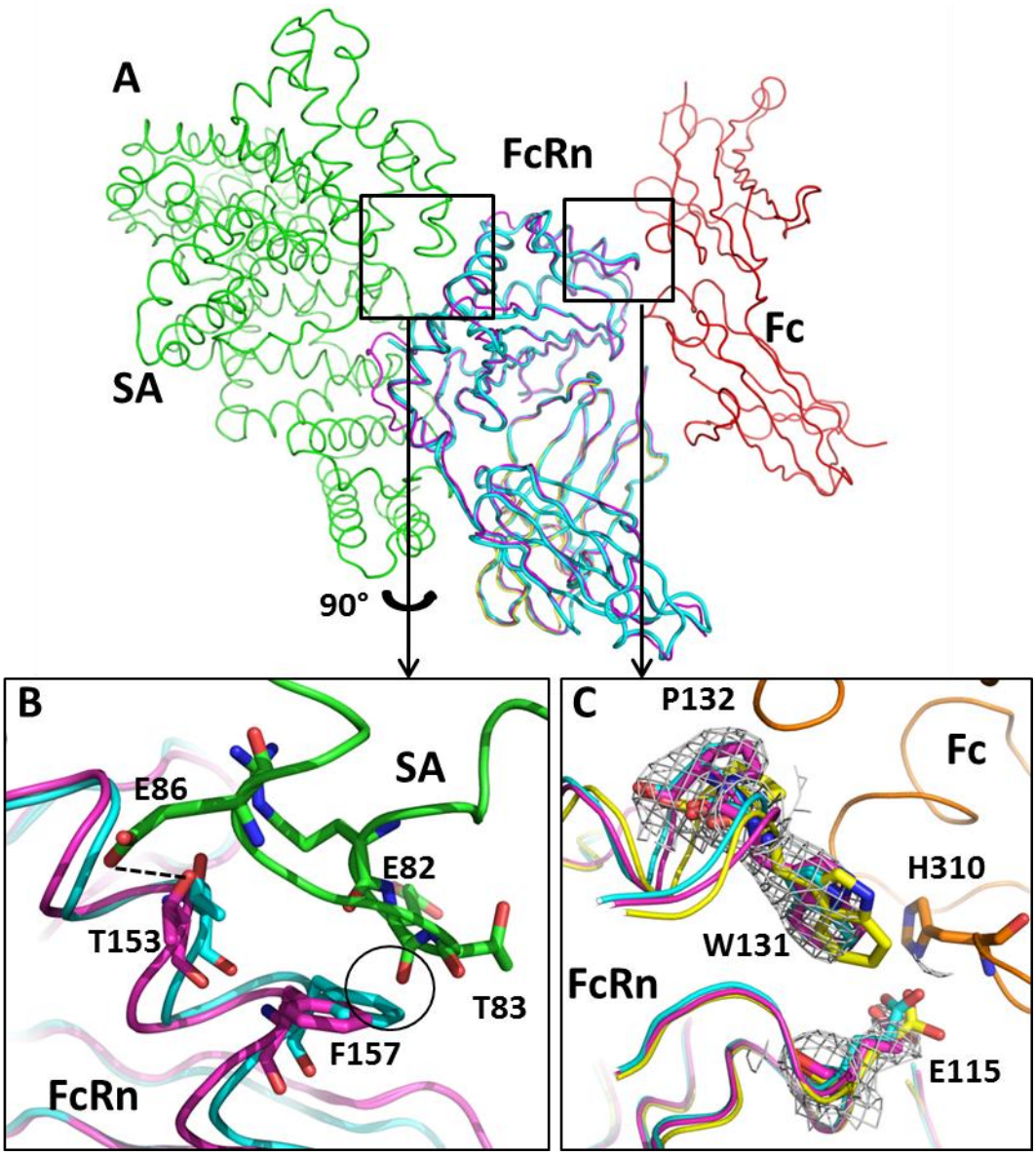

Figure 3. Intermolecular interactions among hFcRn, hSA and Fc and comparisons among the low and high pH unliganded and complex structures. A. Ternary complex structures of hFcRn-hSA-Fc with b-hFcRn superimposed onto the a-hFcRn structures. The boxed regions indicate FcRn-hSA and FcRn-Fc interfaces. B. Zoomed-in view of the FcRn-hSA interface. The carbon atoms in hSA are shown in green, and those of b-hFcRn and a-hFcRn in cyan and magenta, respectively. For clarity, the view is rotated 90° vertically from the boxed view in panel A. The circled region indicates steric clashes between the b-hFcRn and SA, and the dotted line, interactions between FcRn and SA. C. Zoomed-in view of the FcRn-Fc interface. The carbon atoms in Fc are shown in orange, and those of b-hFcRn, a-hFcRn and the ternary complex in cyan, magenta, and yellow, respectively. $2|F_o|-|F_c|$ map of a-hFcRn is shown at the 1 σ level.

ACKNOWLEDGEMENTS

The authors would like to thank Dr. Uta Bussmeyer and Dr. Pankaj Bansal for helpful discussions on baculovirus expression constructs and protein purification methods. We are grateful to the staff at the A1 beamline of Cornell High Energy Synchrotron Source for assistance during X-ray data collection. This work was supported in part by NIH R01 39167 to E. S. W

REFERENCES

[1] Brambell, F. W., The transmission of immune globulins from the mother to the foetal and newborn young. The Proceedings of the Nutrition Society 1969, 28 (1), 35-41.

[2] Pyzik, M.; Rath, T.; Lencer, W. I.; Baker, K.; Blumberg, R. S., FcRn: The Architect Behind the Immune and Nonimmune Func¬tions of IgG and Albumin. Journal of immunology 2015, 194 (10), 4595-4603.

[3] Roopenian, D. C.; Akilesh, S., FcRn: the neonatal Fc receptor comes of age. Nature reviews. Immunology 2007, 7 (9), 715-25.

[4] Burmeister, W. P.; Gastinel, L. N.; Simister, N. E.; Blum, M. L.; Bjorkman, P. J., Crystal structure at 2.2 A resolution of the MHC-related neonatal Fc receptor. Nature 1994, 372 (6504), 336-43.

[5] Simister, N. E.; Mostov, K. E., Cloning and expression of the neonatal rat intestinal Fc receptor, a major histocompatibility complex class I antigen homolog. Cold Spring Harbor symposia on quantitative biology 1989, 54 Pt 1, 571-80.

[6] Simister, N. E.; Rees, A. R., Isolation and characterization of an Fc receptor from neonatal rat small intestine. European journal of immunology 1985, 15 (7), 733-8.

[7] Andersen, J. T.; Foss, S.; Kenanova, V. E.; Olafsen, T.; Leikfoss, I. S.; Roopenian, D. C.; Wu, A. M.; Sandlie, I., Anticarcinoembryonic antigen single-chain variable fragment antibody variants bind mouse and human neonatal Fc receptor with different affinities that reveal distinct cross-species differences in serum half-life. The Journal of biological chemistry 2012, 287 (27), 22927-37.

[8] Martin, W. L.; West, A. P., Jr.; Gan, L.; Bjorkman, P. J., Crystal structure at 2.8 A of an FcRn/heterodimeric Fc complex: mechanism of pH-dependent binding. Molecular cell 2001, 7 (4), 867-77.

[9] Vaughn, D. E.; Bjorkman, P. J., Structural basis of pH-dependent antibody binding by the neonatal Fc receptor. Structure 1998, 6 (1), 63-73.

[10] Chaudhury, C.; Mehnaz, S.; Robinson, J. M.; Hayton, W. L.; Pearl, D. K.; Roopenian, D. C.; Anderson, C. L., The major histocompatibility complex-related Fc receptor for IgG (FcRn) binds albumin and prolongs its lifespan. The Journal of experimental medicine 2003, 197 (3), 315-22.

[11] Oganesyan, V.; Damschroder, M. M.; Cook, K. E.; Li, Q.; Gao, C.; Wu, H.; Dall'Acqua, W. F., Structural insights into neonatal Fc receptor-based recycling mechanisms. The Journal of biological chemistry 2014, 289 (11), 7812-24.

[12] West, A. P., Jr.; Bjorkman, P. J., Crystal structure and immunoglobulin G binding properties of the human major histocompatibility complex-related Fc receptor. Biochemistry 2000, 39 (32), 9698-708.

[13] Schmidt, M. M.; Townson, S. A.; Andreucci, A. J.; King, B. M.; Schirmer, E. B.; Murillo, A. J.; Dombrowski, C.; Tisdale, A. W.; Lowden, P. A.; Masci, A. L.; Kovalchin, J. T.; Erbe, D. V.; Wit-trup, K. D.; Furfine, E. S.; Barnes, T. M., Crystal structure of an HSA/FcRn complex reveals recycling by competitive mimicry of HSA ligands at a pH-dependent hydrophobic interface. Structure 2013, 21 (11), 1966-78.

[14] Mezo, A. R.; Sridhar, V.; Badger, J.; Sakorafas, P.; Nienaber, V., X-ray crystal structures of monomeric and dimeric peptide inhibitors in complex with the human neonatal Fc receptor, FcRn. The Journal of biological chemistry 2010, 285 (36), 27694-701.

[15] Firan, M.; Bawdon, R.; Radu, C.; Ober, R. J.; Eaken, D.; Antohe, F.; Ghetie, V.; Ward, E. S., The MHC class I-related receptor, FcRn, plays an essential role in the maternofetal transfer of gamma-globulin in humans. International immunology 2001, 13 (8), 993-1002.

[16] Otwinowsky, Z.; Minor, W., Processing of X-ray Diffraction Data Collected in Oscillation Mode. In Methods in Enzymology, Carter, J., C. W.; Sweet, R. M., Eds. 1997; Vol. 276, pp 307-326.

[17] Adams, P. D.; Afonine, P. V.; Bunkoczi, G.; Chen, V. B.; Davis, I. W.; Echols, N.; Headd, J. J.; Hung, L. W.; Kapral, G. J.; Grosse-Kunstleve, R. W.; McCoy, A. J.; Moriarty, N. W.; Oeffner, R.; Read, R. J.; Richardson, D. C.; Richardson, J. S.; Terwilliger, T. C.; Zwart, P. H., PHENIX: a comprehensive Python-based system for macromolecular structure solution. Acta crystallographica. Section D, Biological crystallography 2010, 66 (Pt 2), 213-21.

[18] McCoy, A. J.; Grosse-Kunstleve, R. W.; Adams, P. D.; Winn, M. D.; Storoni, L. C.; Read, R. J., Phaser crystallographic software. Journal of applied crystallography 2007, 40 (Pt 4), 658-674.

[19] Emsley, P.; Cowtan, K., Coot: model-building tools for molecular graphics. Acta crystallographica. Section D, Biological crystallography 2004, 60 (Pt 12 Pt 1), 2126-32.

[20] Nicholls, R. A.; Long, F.; Murshudov, G. N., Low-resolution refinement tools in REFMAC5. Acta crystallographica. Section D, Biological crystallography 2012, 68 (Pt 4), 404-17.

[21] Schrodinger, L., The PyMOL Molecular Graphics System, Version 1.3, Schrodinger, LLC. 2010.

[22] Diederichs, K.; Karplus, P. A., Improved R-factors for diffraction data analysis in macromolecular crystallography. Nature structural biology 1997, 4 (4), 269-75.